

 Open access • Posted Content • DOI:10.1101/2020.10.17.343640

Strain population structure varies widely across bacterial species and predicts strain colonization in unrelated individuals — [Source link](#)

[Jeremiah J. Faith](#), [Alice Chen-Liaw](#), [Varun Aggarwala](#), [Nadeem O. Kaakoush](#) ...+8 more authors

Institutions: [Icahn School of Medicine at Mount Sinai](#), [University of New South Wales](#), [St. Vincent's Health System](#), [University of Melbourne](#) ...+3 more institutions

Published on: 17 Oct 2020 - [bioRxiv](#) (Cold Spring Harbor Laboratory)

Topics: [Population](#) and [Population size](#)

Related papers:

- [Fitness estimates from experimental infections predict the long-term strain structure of a vector-borne pathogen in the field.](#)
- [Epidemic clones, oceanic gene pools and eco-LD in the free living marine pathogen *Vibrio parahaemolyticus*](#)
- [Genetic Structure of Natural Populations of *Escherichia coli* in Wild Hosts on Different Continents](#)
- [Genomic diversity of *Escherichia coli* isolates from healthy children in rural Gambia](#)
- [Sex-dependent competitive dominance of phylogenetic group B2 *Escherichia coli* strains within human hosts](#)

Share this paper:    

View more about this paper here: <https://typeset.io/papers/strain-population-structure-varies-widely-across-bacterial-4y475xn3ar>

1 **Strain population structure varies widely across bacterial species and**
2 **predicts strain colonization in unrelated individuals**

3

4 *Jeremiah J. Faith^{1,2*}, Alice Chen-Liaw^{1,2}, Varun Aggarwala^{1,2}, Nadeem O. Kaakoush³, Thomas*
5 *J. Borody⁴, Hazel Mitchell³, Michael A. Kamm^{5,6}, Sudarshan Paramsothy^{7,8}, Evan S. Snitkin⁹,*
6 *and Ilaria Mogno^{1,2}*

7

8 ¹Precision Immunology Institute, Icahn School of Medicine at Mount Sinai, New York, NY 10029,
9 USA

10 ²Icahn Institute for Data Science and Genomic Technology, Icahn School of Medicine at Mount
11 Sinai, New York, NY 10029, USA

12 ³School of Medical Sciences, University of New South Wales, Sydney, NSW 2052, Australia.

13 ⁴Centre for Digestive Diseases, Sydney, NSW 2046, Australia.

14 ⁵Department of Gastroenterology, St Vincent's Hospital, Melbourne, Australia.

15 ⁶Department of Medicine, University of Melbourne, Melbourne, Australia.

16 ⁷Concord Clinical School, University of Sydney, Sydney, NSW 2050, Australia.

17 ⁸Department of Gastroenterology & Hepatology, Macquarie University Hospital, Sydney, NSW
18 2109, Australia.

19 ⁹Department of Microbiology and Immunology, University of Michigan Medical School, Ann Arbor,
20 Michigan, USA.

21

22

23 *Corresponding author: jeremiah.faith@mssm.edu (J.J.F.)

24

25 **Keywords**

26 Gut microbiota, strains, genomics, bacteria

27 **Summary**

28 The population structure of strains within a bacterial species is poorly defined, despite the
29 functional importance of strain variation in the human gut microbiota on health. Here we analyzed
30 >1000 sequenced bacterial strains from the fecal microbiota of 47 individuals from two countries
31 and combined them with >150,000 bacterial genomes from NCBI to quantify the strain population
32 size of different bacterial species, as well as the frequency of finding the same strain colonized in
33 unrelated individuals who had no opportunities for direct microbial strain transmission. Strain
34 population sizes ranged from tens to over one-hundred thousand per species. Prevalent strains
35 in common gut microbiota species with small population sizes were the most likely to be harbored
36 in two or more unrelated individuals. The finite strain population size of certain species creates
37 the opportunity to comprehensively sequence the entirety of these species' prevalent strains and
38 associate their presence in different individuals with health outcomes.

39 Introduction

40 Although it was once unclear if bacterial species could be defined genomically^{1,2}, the recent
41 expansion of bacterial genomes, often with numerous isolates sequenced per species, has
42 enabled genomic bacterial species definitions that empirically reflect or improve existing species
43 names^{3,4}. These species boundaries can be detected in the SNPs of conserved genes (i.e., the
44 average nucleotide identity; ANI)³⁻⁶ and in the large differences in genome overlap (e.g., by
45 pairwise genome alignment) or gene flow discontinuities driven by the strong bias of horizontal
46 gene transfer within a species rather than across species boundaries^{3,7-9}. As in microbial
47 pathogenesis^{10,11}, the functional impact of the microbiome is dependent on strain-level variation
48 within a species¹²⁻¹⁸, which has driven computational advances to track strains¹⁹⁻²², cluster
49 strains²³, measure strain stability^{7,21,24}, and analyze strain variation^{25,26}. Strain-focused algorithms
50 for both the commensal microbiome and infectious disease research have also begun to inform
51 genomic boundaries for bacterial strains^{7,21,22}. Despite the importance of strain-variation, we still
52 lack a broad understanding of the general principles of strain population structure, such as the
53 number of strains in each bacterial species, the stability of these strains²⁷, the prevalence of each
54 strain within a species in human and non-human reservoirs, and the fitness differences and
55 environmental changes that drive alterations in strain prevalence^{27,28}.

56 The study of bacterial pathogens provided the first genomics-based evidence of strain
57 transmission and prevalence across human populations. The strong phenotype induced by both
58 frank bacterial pathogens and colonizing opportunistic bacterial pathogens (COP)²⁹ has facilitated
59 the isolation and genome sequencing of numerous pathogenic isolates, which has demonstrated
60 that pathogens within a given outbreak typically represent one or a small number of genomically-
61 distinct lineages^{10,30-32}. These results demonstrate that the same strain of bacteria can be
62 harbored in multiple unrelated individuals. For many frank bacterial pathogens, this sharing is not
63 through direct human-to-human transfer, but rather the same bacterial strain is colonized in

64 unrelated individuals through the consumption of the same contaminated source (typically food
65 or water).

66 For COP including *Clostridioides difficile* and extraintestinal pathogenic *Escherichia coli*
67 (ExPEC), the colonization of the same strain in unrelated individuals can be both environment-to-
68 human (e.g., shared occupation of a health care facility with insufficiently sterilized equipment) or
69 human-to-human, as these organisms can stably and asymptotically colonize the human gut
70 and act as the reservoir for the recurrent reinfection of the target site of pathogenesis such as in
71 urinary tract infections (UTI)²⁹. Sequencing and isolation efforts for COPs initially focused on
72 outbreak tracking within hospital intensive care units³⁰. They have subsequently demonstrated
73 that multiple COP strains are often asymptotically maintained in long-term care facilities in a
74 complex network of direct and indirect strain sharing³³. COP strains are often multidrug resistant
75 organisms (MDRO) whose antibiotic resistance may in part influence their prevalence in the
76 human population which in turn increases the human risk for COPs. Broader sequencing efforts
77 of MDRO COPs demonstrate that most strains cannot be explained by acquisition at healthcare
78 facilities^{32,34,35} and are likely acquired elsewhere and stably maintained at various prevalence in
79 the healthy human population.

80 Understanding bacterial population structure and strain prevalence, beyond the narrow
81 lens of the hospital environment, could provide novel tools to quantify the association of microbial
82 strains with both infectious and complex human disease, as well as new routes to limit human
83 disease. Early broad explorations of the gut microbiota have demonstrated contexts of enriched
84 strain sharing for commensal microbes including the shared hospital environment for infants²²,
85 fecal microbiota transplantation (FMT)^{19,21}, and early life co-habitation between family
86 members^{7,22}. Although selective pressures likely differ in non-MDRO organisms, the prevalence
87 of a bacterial strain in the broader human microbiota population, beyond enriched scenarios of
88 direct transfer like co-habitation and FMT, is a reflection of a strain's fitness that includes both the
89 transmissibility of the organism and its stability in the host¹³.

90 Here we use a sequenced collection of 2359 bacterial isolates representing 1255 strains
91 that were isolated from the fecal microbiota of 47 individuals from USA and Australia, to study
92 principles of strain population size and their implications for strain-prevalence in unrelated
93 individuals. Strain population size varies dramatically across species with some species being
94 represented by tens of strains and others represented by hundreds of thousands. Prevalent
95 bacterial strains from species with small strain population sizes are far more likely to be colonized
96 in two unrelated individuals than strains from species with large strain population sizes. The finite
97 number of bacterial strains within each species creates the potential to track them and their
98 genetic loci across individuals to identify those associated with short- and long-term health
99 outcomes for both COP pathogenesis and complex disease.

100

101 **Results**

102 **Defining a bacterial strain as a pairwise genome kmer overlap of 0.98 or greater**

103 To better understand the strain population structure of species resident in the human microbiome,
104 we generated a dataset combining 156,403 bacterial genomes from NCBI with 2359 newly
105 sequenced bacterial isolates (hereafter referred to as LOCAL) from 257 species isolated from 47
106 individuals across two countries (USA^{14,21,36} and Australia^{37,38}). We used a k-mer hash-based
107 approach to efficiently calculate the genome overlap between all pairs of bacterial genomes from
108 the same species as the proportion of shared k-mers between the genomes. As in our previous
109 work⁷, we find these species-level genome comparisons are dominated by highly similar (>0.98
110 kmer overlap) genomes when comparing multiple isolates of the same species from a single
111 individual at a single timepoint (Fig. 1A.i) – reflecting the situation where multiple isolates of the
112 same strain are captured and sequenced from the same stool sample. Also similar to our prior
113 work, we find that pairwise comparisons of isolates from the same species that were isolated from
114 one individual at different time points are also dominated by kmer overlaps of >0.98 (Fig. 1A.ii),
115 as these strains are stably maintained over time in each individual and re-isolated at a second

116 time point^{7,39}. Given this strong empirical observation of the kmer overlap of >0.98 between
117 genomes of the same species isolated from an individual, we will use 0.98 as the threshold for
118 defining a bacterial strain for the remaining comparisons across individuals. Performing these
119 analyses with the other popular pairwise genome comparison method of Average Nucleotide
120 Identity (ANI)⁵ yields similar results. However, we find that kmer overlap, which captures both
121 SNPs and gene flow discontinuities⁹, provides improved resolution with less signal saturation
122 between very similar species (Fig. S1A) and better identifies isolates sequenced from the same
123 individual (Fig. S1B).

124

125 **Bacterial strains can colonize different individuals by direct transfer**

126 Although it is clear that pairs of individuals do not typically have large overlaps in their microbiome
127 strain composition, cohabitation and fecal microbiota transplantation provide two possibilities for
128 direct strain transmission between individuals to perhaps increase their strain composition
129 overlap. Comparing the kmer overlap between genomes from the same species isolated from
130 fecal microbiota transplant (FMT) donors and their recipients treated for recurrent *Clostridioides*
131 *difficile* (rCDI)^{40,41}, kmer overlaps >0.98 again dominate, with perhaps slightly more kmer overlaps
132 <0.98 demonstrating the likely acquisition of strains from non-donor (environmental) sources after
133 the transplant (Fig. 1A.iii). These results are in line with our recent observation that the recipient
134 microbiota post-transplant is composed of 80% donor strains, 10% recipient strains (i.e., those
135 colonizing the recipient prior to transplant), and 10% environmentally acquired strains²¹. The
136 second category for an increased chance for direct transmission of bacterial strains is between
137 family members. Although this bacterial transmission is less purposeful than the large microbial
138 biomass transferred in FMT, the cohabitation of individuals provides numerous opportunities for
139 microbial transfer, particularly in early life as the gut microbiota is established¹³. These familial
140 pairwise genome comparisons from isolates of the same species again contained numerous kmer
141 overlaps of >0.98 suggesting familial transfer of bacterial strains as demonstrated in prior studies

142 (Fig. 1A.iv)^{7,42}. Notably, these strain-level kmer overlaps were a minority suggesting direct
143 transmission within families is only a fraction of that experienced via FMT.

144

145 **Bacterial isolates with >0.98 genome kmer overlap can be found in pairs of individuals**
146 **without direct transfer**

147 Although it is clear that factors such as direct transfer of strains via FMT can facilitate strain
148 sharing of commensal bacteria between unrelated individuals and that there is substantial species
149 overlap between individuals, the number of strains in a bacterial species could be sufficiently high
150 or the mutation and recombination rate could be so rapid that it is unlikely to find the same
151 commensal bacterial strains colonized in unrelated individuals inhabiting distal sites of the Earth.
152 We performed pairwise genome kmer overlap comparisons between genomes of the same
153 species from all remaining isolates in our dataset consisting of unrelated individuals where no
154 direct transmission of strains was likely (i.e., no FMT and the individuals are unlikely to have ever
155 had direct contact). We find that the vast majority of comparisons are <0.98 kmer overlap.
156 However, there is a slight, but notable, peak in kmer overlap at an overlap of 0.98 and greater
157 (Fig. 1A.v). This peak could indicate that the population sizes of some common bacterial species
158 are sufficiently small that with our cohort of only 47 individuals we are finding unrelated individuals
159 harboring the same bacterial strain or that convergent evolution within a species pangenome
160 repeatedly drives to a highly similar state.

161

162 **Bacterial strains with >0.98 genome kmer overlap are found for frank pathogens and COP**
163 **pathogens**

164 For comparison with frequent colonization of the same strain in unrelated individuals in complex
165 disease, we calculated the kmer overlap between environmental and human isolates from a
166 spinach outbreak and a “Taco John” outbreak of frank pathogen *Escherichia coli* O157:H7³¹. The
167 mean±std kmer distance of genomes from within each outbreak was 0.982±0.018 and

168 0.985±0.017 for spinach and “Taco John” respectively, while the kmer distance of genomes
169 compared between the two outbreaks was 0.955±0.189. Applying the same method to MDRO
170 COP in the context of carbapenem-resistant *Klebsiella pneumonia* outbreaks in Beijing Tongren
171 hospital³⁰ and Shanghai Huashan hospital⁴³, we found all individuals in the Beijing Tongren
172 outbreak were infected by the same strain (0.996±0.004) while individuals in the Shanghai
173 Huashan outbreak had one of four different strains (0.994±0.004). Similar to the frank pathogens,
174 the kmer distance between independent outbreaks was 0.951±0.020. These results demonstrate
175 that the kmer distance of strains shared in the commensal microbiota can be similar to lineages
176 in pathogen outbreaks.

177

178 **Colonization of the same strain in two unrelated individuals with no direct transfer is more**
179 **prominent when species comparisons are more evenly represented**

180 To further probe the extent to which unrelated individuals might harbor the same bacterial strain,
181 all remaining analyses are focused on pairwise comparisons of LOCAL isolates from the same
182 species between individuals with no direct transfer opportunities (e.g., as in Fig. 1A.v). A caveat
183 of our comparisons in Fig. 1A is that our LOCAL dataset has an uneven number of representatives
184 from each species reflecting both their prevalence in the human population and their ease of
185 bacterial culture. Therefore, in performing all possible pairwise comparisons of isolates in each
186 species, the more common species in the LOCAL dataset will have far more comparisons than
187 those that are rare. To better reflect the kmer overlap distribution across species, we randomly
188 subsampled the pairwise kmer comparisons for each species to have at most the same number
189 of comparisons as the species whose prevalence was the upper quartile LOCAL dataset (Fig.
190 1B). As expected from prior work^{3,7}, organisms from the same species have a characteristic
191 genome overlap where the most common overlap is around 0.70 with increasingly similar kmer
192 overlaps diminishing sharply from kmer overlaps of 0.70 to 0.97 (Fig. 1B). Intriguingly when we
193 use this subsampling approach to include more proportional representation of less frequent

194 species, this decay is followed by a sharp peak of genome kmer overlaps of 0.98 to nearly 1.00.
195 Focusing on all genome kmer overlaps >0.98 grouped by species further reveals that this peak is
196 heavily weighted towards very high genome kmer overlaps of >0.995 with few pairwise
197 comparisons near 0.98 (Fig. S1C). Given the natural decay of genome similarity after 0.70, it
198 seems highly unlikely that this second higher peak occurred by chance. It likely reflects a small
199 subset of strains colonized in multiple unrelated individuals who harbor the same strain but not
200 through direct microbial transmission. These shared strains were found in species for which we
201 have numerous distinct strain isolates and those species with as few as a single unique strain
202 (Fig. 1C) suggesting this observation is not simply an artifact of sampling bias where more
203 prevalent species have more genomes increasing the chance of finding two unrelated individuals
204 with the same strain. Across the ~20,000 pairwise comparisons of LOCAL isolates from the same
205 species between individuals with no direct transfer opportunities, only 0.35% were >0.98 kmer
206 overlap, encompassing 4.67% of the 237 species and 1.35% of the 1255 strains. Amongst all
207 pairwise comparisons of the 47 individuals in the cohort, the chance of a pair of individuals
208 harboring at least one strain that is the same between them was 3.4%, and only one pair of
209 individuals shared two strains that were the same – at the strain level human microbiomes are
210 almost totally unique. While all of the bacterial isolations in the LOCAL dataset were performed in
211 a single anaerobic chamber, these shared strains were often isolated from culture libraries
212 generated years apart, mitigating the chance they represent contaminants.

213

214 **Colonization of the same strain in two unrelated individuals with no direct transfer is**
215 **confirmed in public bacterial genome databases**

216 The large number of publicly available bacterial genomes in NCBI provide an independent dataset
217 to validate the enrichment of genomes with a pairwise kmer overlap of greater than 0.98 in the
218 absence of direct strain transfers between pairs of individuals. While the composition of the strains
219 in NCBI is likely biased towards commercially and medically relevant strains in some species, we

220 can limit these biases to a large extent by comparing the LOCAL bacterial genome to those in
221 NCBI. Although we have limited metadata on the NCBI bacterial genomes, it is highly improbable
222 that the LOCAL strains were isolated from individuals that are first degree relatives or fecal
223 transplant recipients of the individuals whose microbes are in the NCBI genome set. We
224 calculated the kmer overlap of LOCAL bacterial genomes with NCBI bacterial genomes. As in our
225 LOCAL comparisons, the number of representative genomes for each species is highly varied,
226 and we randomly subsampled the pairwise kmer comparisons for each species to have at most
227 the same number of comparisons as the species whose prevalence was the upper quartile in
228 LOCAL dataset (Fig. 1D). We again found a kmer overlap spike between 0.98 and 1.00
229 suggesting the same bacterial strain is found between unrelated individuals in two independent
230 datasets (i.e., within LOCAL and between LOCAL and NCBI) (Fig. 1D). As with the LOCAL
231 pairwise comparisons, we also find for most species that the kmer overlaps >0.98 are heavily
232 biased towards very high overlaps of >0.995 (Fig. S1D). *Enterococcus faecalis* and *Escherichia*
233 *coli* are two notable exceptions to this trend, as their pairwise interactions look more like the true
234 decay of the tail of a distribution rather than a second peak.

235

236 **Strain population sizes vary widely across bacterial species**

237 If unrelated individuals are harboring the same strains of bacteria, it suggests that bacterial
238 species have a finite number of strains (i.e., a population size) that are stably maintained and
239 propagated in the human population. In both macro- and microecology, it is often impossible to
240 exhaustively sample a population to determine its size (also known as total taxonomic richness).
241 Two approaches are commonly used to infer population sizes from a subsample of its members.
242 One of these approaches takes a subsample of the population (e.g., the set of strains in species
243 *Bacteroides ovatus* in NCBI) and quantifies the frequency distribution of population members
244 found once, twice, etc.. as f_1, f_2, \dots, f_N (Fig. 2A). If the population is not exhaustively sampled,
245 there exists an unobserved group f_0 that has not yet been detected in the subsample, which can

246 be inferred from the data (e.g., the number of unique *B. ovatus* strains that have not yet been
247 isolated and sequenced)⁴⁴. After inferring f_0 , the population size can then be calculated as the
248 sum of the observed and unobserved community members with the assumption in our case that
249 the number of strains within a species at any time (or within the timescale of human lifetimes) is
250 finite. We applied the iChao algorithm of Chui and Chao⁴⁵ that uses Hill statistics to estimate strain
251 population sizes. To focus on the gut microbiome and species where this inference would be most
252 robust, we calculated strain population sizes for the species in LOCAL that had at least 50 genome
253 sequences in NCBI and that were found shared within LOCAL or between LOCAL and NCBI.
254 Across these species, we inferred vastly different population sizes across a >9000-fold range with
255 19 as the smallest strain population estimated for *Bifidobacterium animalis* and 1.8×10^5 estimated
256 for *Escherichia coli* (Table 1).

257 Mark and recapture methods provide an alternative method to estimate population size by
258 using two consecutive subsamples of a population. In the first sampling, the “captured” members
259 are marked and released back into the population. In the second sampling, one will observe some
260 new members and potentially some “recaptured” members that were marked in the previous
261 round. Population size can be estimated from the number of members collected in each of the
262 two subsamplings and the proportion of marked and unmarked community members resampling
263 (e.g., using the Chapman algorithm⁴⁶). To apply this alternative method of calculating population
264 size, we assume the genomes in NCBI represent the initial sampling and the LOCAL genomes
265 represent the resampling. Like the frequency distribution approach above, the mark and recapture
266 approach estimated vastly different population sizes over a >9000-fold range with 10 as the
267 smallest strain population estimated for *Bifidobacterium animalis* and 9.2×10^4 for *Escherichia coli*
268 (Table 1). The log of the strain population sizes for each species estimated with these two different
269 approaches were highly correlated ($r=0.91$; $p=2.9 \times 10^{-6}$; Fig. 2B) suggesting they roughly
270 approximate the true strain population size of each species.

271 Given the large variation in strain population size across species, our probability of
272 observing indirect strain sharing, within a species between two individuals, will be influenced by
273 the population size for that species. As expected, we find a significant negative correlation
274 between the log proportion of strains shared within a species in LOCAL and the log population
275 size for the species ($r = -0.95$; $p=2.8 \times 10^{-4}$; Fig. 2C top plot) as well as between log proportion of
276 strains shared between LOCAL and NCBI for a given species ($r = -0.81$; $p=2.4 \times 10^{-4}$; Fig. 2C
277 bottom plot). For example, *B. animalis* had a population size of 19 estimated from 66 genomes
278 from 9 unique strains in NCBI. In LOCAL, *B. animalis* had single unique strain that colonized
279 seven different individuals, five individuals in the USA and two individuals in Australia.

280 Just as more favorable genetic alleles expand in the human population, we would expect
281 the frequency distribution of strains within a bacterial species to be uneven and in proportion to
282 the fitness of each strain with the most transmissible and stable strains dominating the species.
283 These more frequent strains within a species would similarly have an increased chance of being
284 found in two unrelated individuals. To test this hypothesis, for each species shared between
285 LOCAL and NCBI we compared the unweighted proportion of the strain within the species in NCBI
286 to the weighted prevalence of the strain in the species in NCBI, where the weighted prevalence
287 is defined by the frequency of the strain in NCBI. For example, we found one of the nine *B.*
288 *animalis* strains in NCBI was shared with LOCAL (11%). However, since this shared strain was
289 also the most prevalent *B. animalis* strain in NCBI (51 out of 66 genomes), it represented 77% of
290 the *B. animalis* genomes in NCBI. It was similarly the case for all but one (*S. oralis*) of the 14
291 shared strains between LOCAL and NCBI that the shared strains represented more prevalent
292 strains within a given species ($p=0.026$; paired t-test; Fig. 2D). This bias towards indirect sharing
293 of prevalent strains can also be seen in Fig. 2A where the strain frequency in NCBI is highlighted
294 in red for strains that are shared between NCBI and LOCAL. The red points are skewed towards
295 the right showing that the more prevalent strains were more likely to be found indirectly shared
296 between the two datasets.

297

298 **Discussion**

299 Overall, we have identified numerous instances of the same bacterial strain harbored in two
300 different individuals without a direct microbial transmission event. These results suggest the
301 number of strains in at least some bacterial species can be finite and stably maintained in the
302 human population where they colonize unrelated individuals across the world⁴⁷. Predictably,
303 common species with smaller population sizes were more likely to be found shared between
304 individuals. Finally, strains were unevenly distributed within each species with presumably more
305 fit strains being more prevalent in the population and more likely to be found in unrelated
306 individuals.

307 Although genetic diversity is generated in bacteria through mutation and horizontal gene
308 transfer and the strains within a community will drift as one or more stable substrains over time³⁹,
309 for many species the genetic boundary of 98% genome similarity appears to be retained at least
310 on human health relevant time scales. Here we observed this phenomenon in the incredibly
311 similar kmer overlaps between the strains shared between LOCAL and NCBI. For example, one
312 shared strain of *Lacticaseibacillus rhamnosus* has a kmer overlap of 0.9994 with the type strain
313 isolated >30 years ago⁴⁸ and a shared strain of *Ligilactobacillus salivarius* has a kmer overlap of
314 0.9988 with a strain isolated >60 years ago⁴⁹.

315 Notably, the strains harbored in pairs of unrelated individuals in LOCAL or between
316 LOCAL and NCBI were limited to only 16 total species out of the 237 in our cohort. Species with
317 the smallest strain populations were often ones used in probiotics, suggesting their small
318 population size might have resulted from direct human intervention limiting strain diversity and
319 increasing the prevalence of certain strains. Other species with smaller populations of strains
320 were microbes that are found more commonly in other habitats including skin origin
321 (Staphylococci)⁵⁰ and oral origin (Streptococci). These organisms were perhaps transient
322 components of the fecal microbiota, from the individual's microbiome, that were enriched by

323 selective media used to culture each fecal microbiome. This result might suggest that average
324 strain population sizes will differ for species enriched in different habitats. Of the four dominant
325 phyla of the human gut microbiota (Firmicutes, Bacteroidetes, Actinobacteria, and
326 Proteobacteria), only Bacteroidetes were never found to be indirectly shared in our analyses,
327 perhaps because the number of currently sequenced strains for all species in this phylum in both
328 NCBI and LOCAL is low. Amongst the tested species in our analyses, only 4% and 13% of those
329 with <10 unique strains and 10-100 unique strains respectively in NCBI were found to have a
330 shared strain with LOCAL, while 50% of species with ≥ 100 unique NCBI strains had a shared
331 strain with LOCAL. Alternatively, perhaps the decaying tail of pairwise kmer overlap of *E. coli* (Fig.
332 S1C and S1D) is a signature suggestive of an organism whose recombination and mutation rates
333 are too fast to have a finite population size. Increased numbers of sequenced Bacteroidetes
334 isolates in the coming years will reveal if a similar decay occurs for strains of species in this
335 phylum.

336 The identification of finite bacterial strain populations suggests that for some species we
337 might be able to approach a complete sequencing of all strains. This sequencing effort combined
338 with strain tracking algorithms to identify the frequency of each strain in shallow metagenomics
339 datasets²¹ from tens of thousands of individuals could facilitate the association of specific
340 bacterial strains with human health and disease to complement gene-based associations. Since
341 the most frequent strains will likely be isolated first, this initiative would enable association of
342 health outcomes with the most prevalent human associated microbes and enable studies to
343 understand factors driving strain prevalence in the human population.

344 **Methods**

345 **Bacterial genomes**

346 Bacteria were isolated as previously described^{14,36}. All bacterial genomes from the LOCAL cohort
347 were sequenced with an Illumina HiSeq2500 or HiSeq4000. The NCBI RefSeq 156,403 bacterial
348 genomes set was downloaded on May 27, 2019 using filters to exclude: partial genomes, derived
349 environmental sources, derived metagenome, derived from single cell, genome length too large,
350 genome length too small, high contig L50, low contig N50, low quality sequence, many
351 frameshifted proteins, and anomalous.

352

353 **Quantifying kmer distances and average nucleotide identity (ANI)**

354 The kmer overlap between any two genomes A and B was determined by generating a hash for
355 genome A with kmer size 20 and quantifying the proportion of kmers shared in both genomes A
356 and B divided by the total number of kmers in A. These distances were independently calculated
357 in both directions. Given the focus of this manuscript on species and strain-level distances,
358 particularly those of kmer overlap >0.98, we initially calculated the kmer overlap for the first 50,000
359 kmers in each genome and only performed the full genome comparison when this initial kmer
360 coverage was >0.1. ANI was calculated using the fastANI algorithm⁵.

361

362 **Estimation of bacterial strain population sizes for each species**

363 The frequency distribution of strain genomes that were found once, twice, etc.. for a given species
364 as f_1, f_2, \dots, f_N was determined by quantifying all pairwise genome kmer distances between all
365 156,403 genomes in the NCBI cohort. Given the large number of pairwise distances, genomes
366 were clustered at the strain-level with a greedy heuristic algorithm that joined a genome into the
367 cluster if any other genome in the cluster had >0.98 kmer overlap. The frequencies of f_1, f_2, \dots, f_N
368 were calculated as the number of clusters of size 1, 2, ..., N respectively. Population sizes
369 estimated from these frequencies were calculated using the iChao algorithm based on Hill

370 statistics. Population sizes estimated with the Mark and Recapture approach were estimated with
371 the Chapman estimator $N_S = \frac{(K_S+1)(n_S+1)}{(k_S+1)} - 1$ where N_S is the number of strains in the population
372 for species S , n_S is the number of unique strains in the NCBI dataset for species S , k_S is the
373 number of species S strains in the LOCAL dataset that were also find in the NCBI database, and
374 K_S is the number of strains from species S in the LOCAL dataset.

375

376 **Data and code availability**

377 Bacterial genomes for this study are available via NCBI BioProject PRJNA637878.

378

379 **Acknowledgments**

380 This work was supported in part by the staff and resources of the Microbiome Translational Center
381 and the Scientific Computing Division in Icahn School of Medicine at Mount Sinai. This work was
382 supported by National Institutes of Health Grants (NIDDK DK112978 and NIDDK DK114133).

383

384 **Author contributions**

385 J.J.F conceived the study and designed the experiments; E.S.S provided insights from infectious
386 disease; I.M. developed the high throughput culturing and genome sequencing infrastructure.
387 N.O.K., T.J.B., H.M., M.A.K., and S.P. collected Australian stool samples; I.M., A.C.L., and Z.L.
388 isolated and sequenced the bacterial genomes; J.J.F., I.M., E.S.S. and V.A. analyzed data; J.J.F.
389 wrote the manuscript. All authors read and approved the final manuscript.

390

391 **Declaration of interests**

392 The authors declare no conflict of interests.

393

394 **References**

- 395 1. Gevers, D. *et al.* Opinion: Re-evaluating prokaryotic species. *Nat. Rev. Microbiol.* **3**,
396 733–739 (2005).
- 397 2. Goldenfeld, N. & Woese, C. Biology's next revolution. *Nature* **445**, 369 (2007).
- 398 3. Varghese, N. J. *et al.* Microbial species delineation using whole genome sequences.
399 *Nucleic Acids Res.* **43**, 6761–6771 (2015).
- 400 4. Mende, D. R., Sunagawa, S., Zeller, G. & Bork, P. Accurate and universal delineation of
401 prokaryotic species. *Nat. Methods* **10**, 881–884 (2013).
- 402 5. Jain, C., Rodriguez-R, L. M., Phillippy, A. M., Konstantinidis, K. T. & Aluru, S. High
403 throughput ANI analysis of 90K prokaryotic genomes reveals clear species boundaries.
404 *Nat. Commun.* **9**, 5114 (2018).
- 405 6. Olm, M. R. *et al.* Consistent Metagenome-Derived Metrics Verify and Delineate
406 Bacterial Species Boundaries. *mSystems* **5**, e00731-19, /msystems/5/1/msys.00731-
407 19.atom (2020).
- 408 7. Faith, J. J. *et al.* The long-term stability of the human gut microbiota. *Science* **341**,
409 1237439 (2013).
- 410 8. Fraser, C., Alm, E. J., Polz, M. F., Spratt, B. G. & Hanage, W. P. The bacterial species
411 challenge: making sense of genetic and ecological diversity. *Science* **323**, 741–746
412 (2009).
- 413 9. Arevalo, P., VanInsberghe, D., Elsherbini, J., Gore, J. & Polz, M. F. A Reverse Ecology
414 Approach Based on a Biological Definition of Microbial Populations. *Cell* **178**, 820-
415 834.e14 (2019).

- 416 10. Snitkin, E. S. *et al.* Tracking a Hospital Outbreak of Carbapenem-Resistant *Klebsiella*
417 pneumoniae with Whole-Genome Sequencing. *Sci. Transl. Med.* **4**, 148ra116-148ra116
418 (2012).
- 419 11. Blaser, M. J. *et al.* Infection with *Helicobacter pylori* strains possessing *cagA* is
420 associated with an increased risk of developing adenocarcinoma of the stomach.
421 *Cancer Res.* **55**, 2111–2115 (1995).
- 422 12. Arthur, J. C. *et al.* Intestinal Inflammation Targets Cancer-Inducing Activity of the
423 Microbiota. *Science* **338**, 120–123 (2012).
- 424 13. Faith, J. J., Colombel, J.-F. & Gordon, J. I. Identifying strains that contribute to complex
425 diseases through the study of microbial inheritance. *Proc. Natl. Acad. Sci. U. S. A.* **112**,
426 633–640 (2015).
- 427 14. Yang, C. *et al.* Fecal IgA Levels Are Determined by Strain-Level Differences in
428 *Bacteroides ovatus* and Are Modifiable by Gut Microbiota Manipulation. *Cell Host*
429 *Microbe* **27**, 467-475.e6 (2020).
- 430 15. Britton, G. J. *et al.* Microbiotas from Humans with Inflammatory Bowel Disease Alter the
431 Balance of Gut Th17 and ROR γ t+ Regulatory T Cells and Exacerbate Colitis in Mice.
432 *Immunity* **50**, 212-224.e4 (2019).
- 433 16. Kittana, H. *et al.* Commensal *Escherichia coli* Strains Can Promote Intestinal
434 Inflammation via Differential Interleukin-6 Production. *Front. Immunol.* **9**, 2318 (2018).
- 435 17. Viladomiu, M. *et al.* IgA-coated *E. coli* enriched in Crohn's disease spondyloarthritis
436 promote TH17-dependent inflammation. *Sci. Transl. Med.* **9**, (2017).
- 437 18. Glasser, A. L. *et al.* Adherent invasive *Escherichia coli* strains from patients with Crohn's
438 disease survive and replicate within macrophages without inducing host cell death.
439 *Infect. Immun.* **69**, 5529–5537 (2001).

- 440 19. Smillie, C. S. *et al.* Strain Tracking Reveals the Determinants of Bacterial Engraftment in
441 the Human Gut Following Fecal Microbiota Transplantation. *Cell Host Microbe* **23**, 229-
442 240.e5 (2018).
- 443 20. Li, S. S. *et al.* Durable coexistence of donor and recipient strains after fecal microbiota
444 transplantation. *Science* **352**, 586–589 (2016).
- 445 21. Aggarwala, V. *et al.* *Quantification of discrete gut bacterial strains following fecal*
446 *transplantation for recurrent Clostridioides difficile infection demonstrates long-term*
447 *stable engraftment in non-relapsing recipients.*
448 <http://biorxiv.org/lookup/doi/10.1101/2020.09.10.292136> (2020)
449 doi:10.1101/2020.09.10.292136.
- 450 22. Olm, M. R. *et al.* *InStrain enables population genomic analysis from metagenomic data*
451 *and rigorous detection of identical microbial strains.*
452 <http://biorxiv.org/lookup/doi/10.1101/2020.01.22.915579> (2020)
453 doi:10.1101/2020.01.22.915579.
- 454 23. Truong, D. T., Tett, A., Pasolli, E., Huttenhower, C. & Segata, N. Microbial strain-level
455 population structure and genetic diversity from metagenomes. *Genome Res.* **27**, 626–
456 638 (2017).
- 457 24. Schloissnig, S. *et al.* Genomic variation landscape of the human gut microbiome. *Nature*
458 **493**, 45–50 (2013).
- 459 25. Poyet, M. *et al.* A library of human gut bacterial isolates paired with longitudinal
460 multiomics data enables mechanistic microbiome research. *Nat. Med.* **25**, 1442–1452
461 (2019).
- 462 26. Vatanen, T. *et al.* Genomic variation and strain-specific functional adaptation in the
463 human gut microbiome during early life. *Nat. Microbiol.* **4**, 470–479 (2019).

- 464 27. Kallonen, T. *et al.* Systematic longitudinal survey of invasive *Escherichia coli* in England
465 demonstrates a stable population structure only transiently disturbed by the emergence
466 of ST131. *Genome Res.* (2017) doi:10.1101/gr.216606.116.
- 467 28. Corander, J. *et al.* Frequency-dependent selection in vaccine-associated pneumococcal
468 population dynamics. *Nat. Ecol. Evol.* **1**, 1950–1960 (2017).
- 469 29. Price, L. B., Hungate, B. A., Koch, B. J., Davis, G. S. & Liu, C. M. Colonizing
470 opportunistic pathogens (COPs): The beasts in all of us. *PLoS Pathog.* **13**, e1006369
471 (2017).
- 472 30. Sui, W. *et al.* Whole genome sequence revealed the fine transmission map of
473 carbapenem-resistant *Klebsiella pneumoniae* isolates within a nosocomial outbreak.
474 *Antimicrob. Resist. Infect. Control* **7**, 70 (2018).
- 475 31. Eppinger, M., Mammel, M. K., Leclerc, J. E., Ravel, J. & Cebula, T. A. Genomic
476 anatomy of *Escherichia coli* O157:H7 outbreaks. *Proc. Natl. Acad. Sci. U. S. A.* **108**,
477 20142–20147 (2011).
- 478 32. Hawken, S. E. & Snitkin, E. S. Genomic epidemiology of multidrug-resistant Gram-
479 negative organisms. *Ann. N. Y. Acad. Sci.* **1435**, 39–56 (2019).
- 480 33. Ciccolini, M. *et al.* Infection prevention in a connected world: the case for a regional
481 approach. *Int. J. Med. Microbiol. IJMM* **303**, 380–387 (2013).
- 482 34. Mellmann, A. *et al.* Real-Time Genome Sequencing of Resistant Bacteria Provides
483 Precision Infection Control in an Institutional Setting. *J. Clin. Microbiol.* **54**, 2874–2881
484 (2016).
- 485 35. Roach, D. J. *et al.* A Year of Infection in the Intensive Care Unit: Prospective Whole
486 Genome Sequencing of Bacterial Clinical Isolates Reveals Cryptic Transmissions and
487 Novel Microbiota. *PLoS Genet.* **11**, e1005413 (2015).

- 488 36. Britton, G. J. *et al.* Defined microbiota transplant restores Th17/ROR γ t+ regulatory T cell
489 balance in mice colonized with inflammatory bowel disease microbiotas. *Proc. Natl.*
490 *Acad. Sci. U. S. A.* **117**, 21536–21545 (2020).
- 491 37. Paramsothy, S. *et al.* Specific Bacteria and Metabolites Associated With Response to
492 Fecal Microbiota Transplantation in Patients With Ulcerative Colitis. *Gastroenterology*
493 **156**, 1440-1454.e2 (2019).
- 494 38. Paramsothy, S. *et al.* Multidonor intensive faecal microbiota transplantation for active
495 ulcerative colitis: a randomised placebo-controlled trial. *Lancet Lond. Engl.* **389**, 1218–
496 1228 (2017).
- 497 39. Zhao, S. *et al.* Adaptive Evolution within Gut Microbiomes of Healthy People. *Cell Host*
498 *Microbe* **25**, 656-667.e8 (2019).
- 499 40. Hirten, R. P. *et al.* Microbial Engraftment and Efficacy of Fecal Microbiota Transplant for
500 Clostridium Difficile in Patients With and Without Inflammatory Bowel Disease. *Inflamm.*
501 *Bowel Dis.* **25**, 969–979 (2019).
- 502 41. Contijoch, E. J. *et al.* Gut microbiota density influences host physiology and is shaped
503 by host and microbial factors. *eLife* **8**, (2019).
- 504 42. Goodman, K. J. & Correa, P. Transmission of Helicobacter pylori among siblings.
505 *Lancet Lond. Engl.* **355**, 358–362 (2000).
- 506 43. Chen, C. *et al.* Tracking Carbapenem-Producing Klebsiella pneumoniae Outbreak in an
507 Intensive Care Unit by Whole Genome Sequencing. *Front. Cell. Infect. Microbiol.* **9**, 281
508 (2019).
- 509 44. Bunge, J., Willis, A. & Walsh, F. Estimating the Number of Species in Microbial Diversity
510 Studies. *Annu. Rev. Stat. Its Appl.* **1**, 427–445 (2014).
- 511 45. Chiu, C.-H. & Chao, A. Distance-Based Functional Diversity Measures and Their
512 Decomposition: A Framework Based on Hill Numbers. *PLoS ONE* **9**, e100014 (2014).

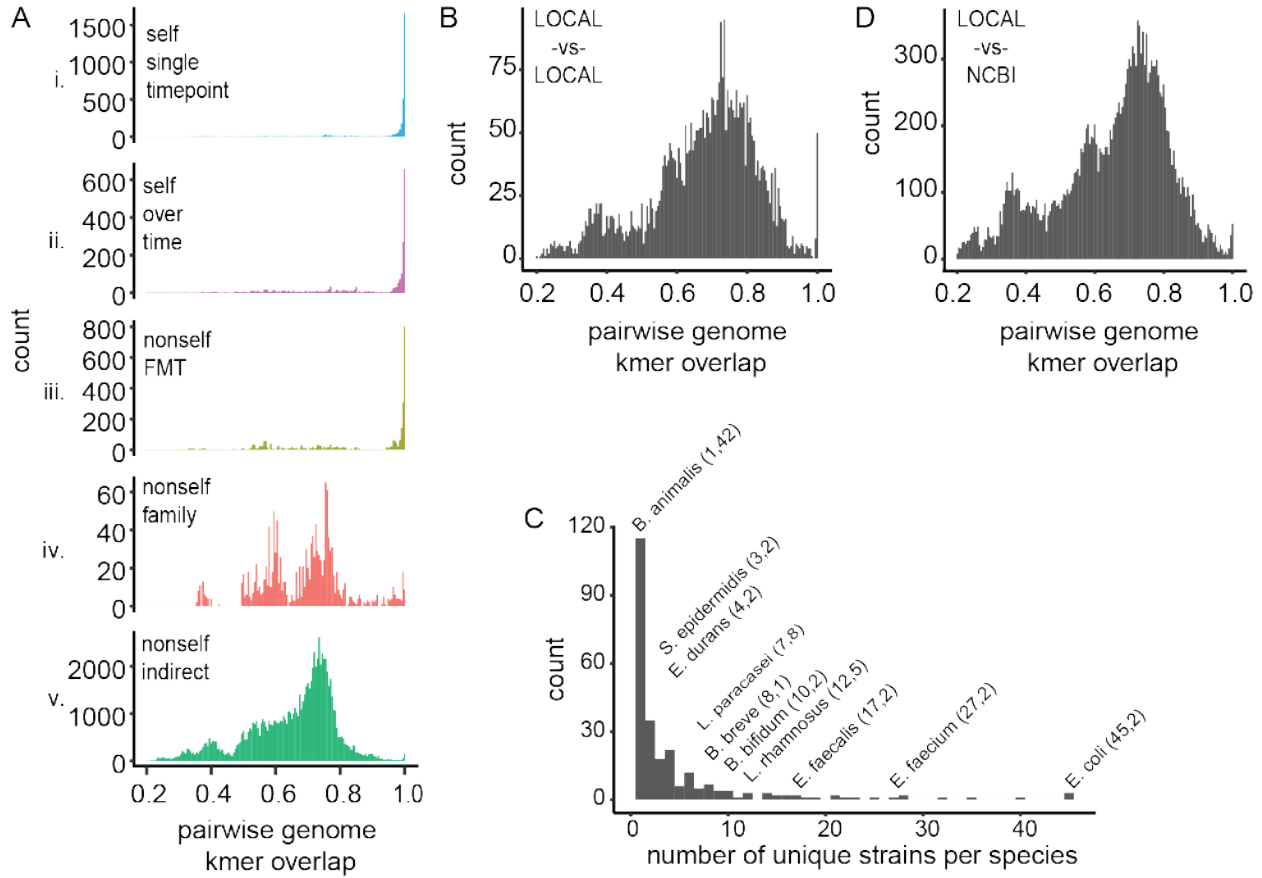
- 513 46. Chapman, D.G. *Some properties of the hypergeometric distribution with applications to*
514 *zoological sample censuses*. (Berkeley, University of California Press, 1951).
- 515 47. Garud, N. R. & Pollard, K. S. Population Genetics in the Human Microbiome. *Trends*
516 *Genet. TIG* **36**, 53–67 (2020).
- 517 48. Collins, Matthew D., Phillips, Brian A. & Zanoni, Paolo. Deoxyribonucleic Acid Homology
518 Studies of *Lactobacillus casei*, *Lactobacillus paracasei* sp. nov., subsp. *paracasei* and
519 subsp. *tolerans*, and *Lactobacillus rhamnosus* sp. nov., comb. nov. *Int. J. Syst.*
520 *Bacteriol.* **39**, 105–108 (1989).
- 521 49. Rogosa, M., Wiseman, R. F., Mitchell, J. A., Disraely, M. N. & Beaman, A. J. Species
522 differentiation of oral lactobacilli from man including description of *Lactobacillus*
523 *salivarius* nov spec and *lactobacillus Cellobiosus* nov spec. *J. Bacteriol.* **65**, 681–699
524 (1953).
- 525 50. Byrd, A. L. *et al.* *Staphylococcus aureus* and *Staphylococcus epidermidis* strain diversity
526 underlying pediatric atopic dermatitis. *Sci. Transl. Med.* **9**, (2017).
- 527
- 528
- 529

530 **Table 1. Strain population sizes for bacterial species.**
531

species	LOCAL strains	NCBI genomes	NCBI strains	shared strains LOCAL		
				with NCBI	iChao	Chapman
<i>Bifidobacterium animalis</i>	1	66	9	1	19	10
<i>Bifidobacterium bifidum</i>	10	65	38	1	72	215
<i>Bifidobacterium breve</i>	8	96	68	2	247	207
<i>Citrobacter freundii</i>	4	269	213	1	1907	535
<i>Enterococcus durans</i>	4	22	19	0	161	NA
<i>Enterococcus faecalis</i>	17	1146	594	6	2579	1530
<i>Enterococcus faecium</i>	27	2558	1698	2	16945	15857
<i>Escherichia coli</i>	45	27160	18099	8	179012	92511
<i>Lactobacillus paracasei</i>	7	172	124	5	28	167
<i>Lactobacillus plantarum</i>	8	445	203	2	74	612
<i>Lactobacillus rhamnosus</i>	12	160	50	6	70	95
<i>Lactobacillus salivarius</i>	5	84	57	1	28	174
<i>Staphylococcus aureus</i>	1	10646	425	1	302	426
<i>Staphylococcus epidermidis</i>	3	636	215	0	105	NA
<i>Streptococcus agalactiae</i>	3	1118	192	2	180	257
<i>Streptococcus mutans</i>	7	195	126	3	85	254
<i>Streptococcus oralis</i>	4	127	115	0	20	NA

532

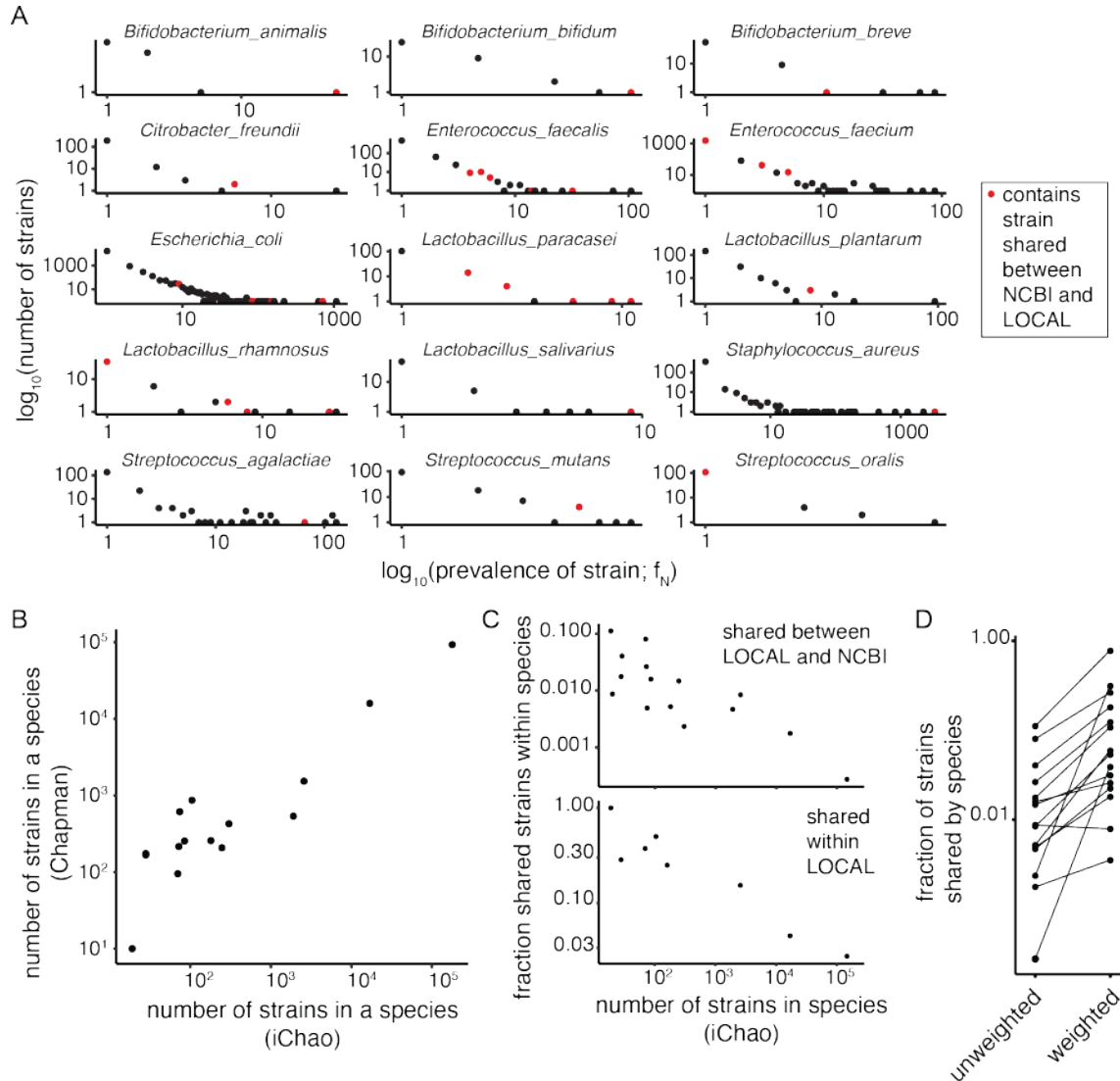
533 **Figures and legends**



534

535 **Figure 1. Highly similar bacterial species are enriched in the context of cohabitation and**
 536 **transmission but not absent in all unrelated individuals with no direct contact. (A)** The
 537 shared kmer content was calculated for all pairwise combinations of species between (i)
 538 individuals' own microbes from a single sample, (ii) individuals' own microbes from two different
 539 timepoint, (iii) FMT donors and their recipients, (iv) members of the same family, (v) two unrelated
 540 individuals with no opportunities for direct microbial transfer between them. (B) A randomly
 541 subsampled set of all pairwise species kmer overlap between genomes from 47 different
 542 individuals reveals a peak at kmer distance >0.98 even when eliminating strains assumed to be
 543 shared by direct transmission (FMT) or cohabitation (family). (C) The strains indirectly shared in
 544 LOCAL were from nine different bacterial species with varying numbers of strains in our genome
 545 set. For species labels on pane C, the first integer is the number of unique strains for a given

546 species in LOCAL, while the second integer is the number of pairwise observations of the same
547 strain in two unrelated individuals with no direct transfer event. **(D)** A similar high kmer overlap
548 >0.98 peak was observed between LOCAL genomes and NCBI genomes.



549

550 **Figure 2. Strain population size varies by species and predicts the frequency of strain**

551 **sharing between unrelated individuals with no direct microbial transmission. (A)** Strains in

552 NCBI are present at different frequencies with the largest number of strains present only a single

553 time and a few prevalent strains that are much more highly represented in the species' population

554 sample of genomes available from NCBI. **(B)** Estimation of strain populations for bacterial species

555 is highly correlated when using either a strain frequency approach (iChao) using only genomes

556 from NCBI or a mark and recapture method (Chapman) that considers the proportion of LOCAL

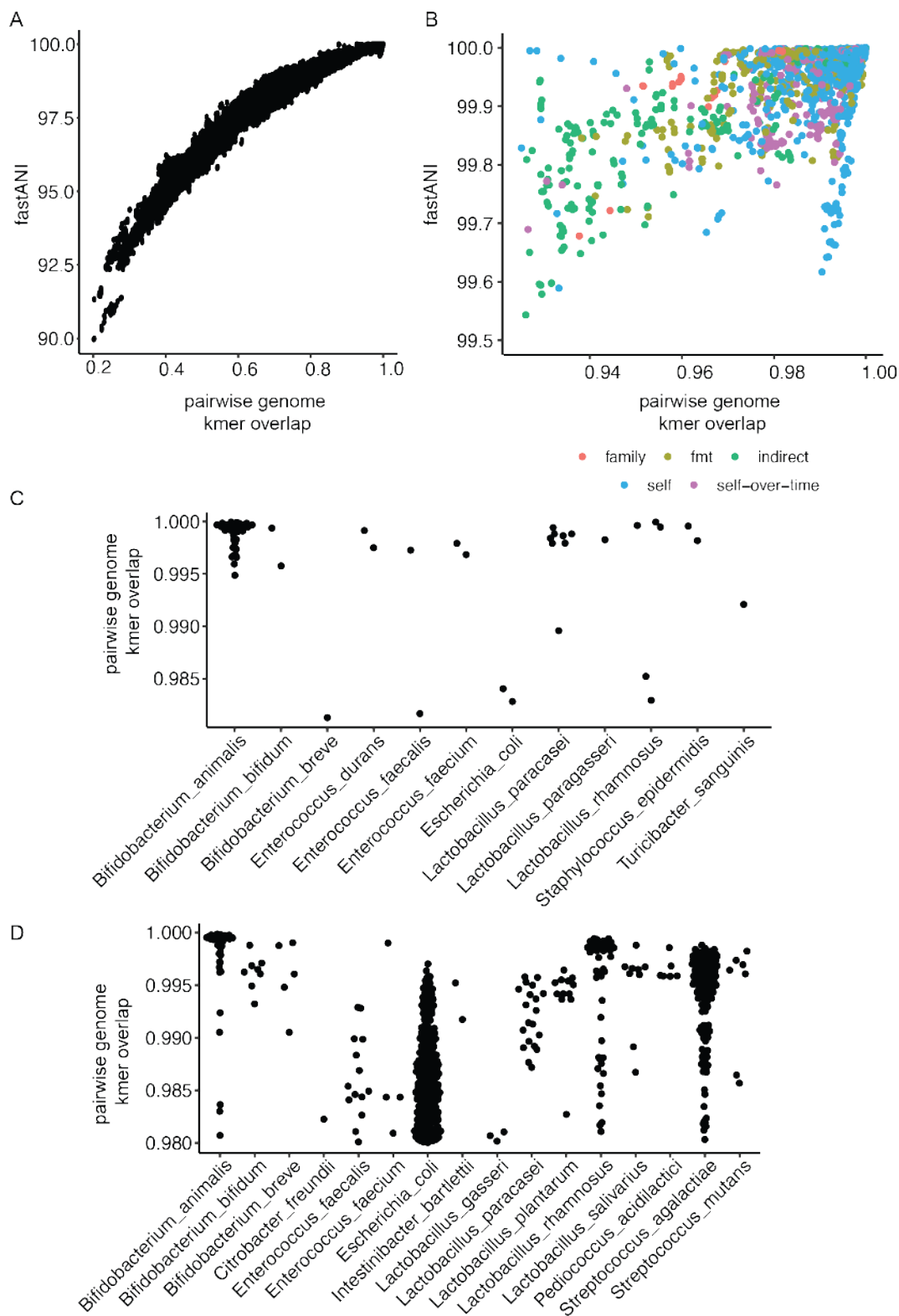
557 strains found in NCBI. **(C)** The strain population size of each species is highly predictive of the

558 fraction of indirect strain sharing between LOCAL and NCBI (top pane) and indirect sharing within

559 LOCAL (bottom pane). **(D)** The unweighted proportion of NCBI strains shared with LOCAL is the
560 proportion of NCBI strains shared with LOCAL weighted by strain prevalence.

561

562



563

564 **Figure S1. Comparing genome similarity metrics and observing the extreme tail of the kmer**

565 **overlap distribution. (A) Overall, genome similarities measured with fastANI and kmer overlap**

566 are highly correlated with the fastANI metric appearing to approach saturation in resolving very
567 similar genomes from the same species. **(B)** Empirically, the kmer overlap metric of >0.98 seems
568 to delineate self-vs-self comparisons (magenta and blue points) more consistently than fastANI.
569 **(C,D)** With few exceptions the kmer overlap comparisons >0.98 for each species are skewed
570 towards kmer overlaps > 0.99.